Hindawi Publishing Corporation
Journal of Nanomaterials
Volume 2015, Article ID 103689, 5 pages
http://dx.doi.org/10.1155/2015/103689

Research Article

$Sr_{2-x}Ba_xTiO_4:Eu^{3+}$, Gd^{3+}: A Novel Blue Converting Yellow-Emitting Phosphor for White Light-Emitting Diodes

Limin Dong,[1,2] Jiatong Zhao,[1] Qin Li,[1] and Zhidong Han[1,2]

[1]*College of Materials Science and Engineering, Harbin University of Science and Technology, Harbin 150040, China*
[2]*Key Laboratory of Engineering Dielectrics and Its Application, Ministry of Education, Harbin University of Science and Technology, Harbin 150040, China*

Correspondence should be addressed to Limin Dong; donglimin@hrbust.edu.cn

Received 19 May 2015; Accepted 27 August 2015

Academic Editor: Sami U. Rather

A highly intense yellow-emitting phosphor $Sr_{2-x}Ba_xTiO_4:Eu^{3+}$, Gd^{3+} peaking at 593–611 nm was synthesized by the sol-gel method. XRD and SEM show that the samples are single phase and have irregular shape. The excitation wavelength matches well with that of the emission of the blue-light-emitting diode. The emission peaks at 593 and 611 nm are attributed to the transitions from the $^5D_0$-$^7F_1$ and $^5D_0$-$^7F_2$ of Eu^{3+} ions, respectively. Gd^{3+} was used as sensitizer, aiming at increasing the luminous intensity. A certain amount of Sr^{2+} and Ba^{2+} is contributed to the intensity of light emission.

1. Introduction

A light revolution is sweeping all over the world due to its advanced properties such as long life time, low energy consumption, high efficiency, environmental friendliness, and the potential applications in indicators, backlights, automobile head-lights, and general illuminations [1, 2]. In the context of energy and environmental protection, the development of LED is taken into consideration. Currently, there are three main methods for WLED technology: blue chip and yellow phosphor approach; tricolor LED chip direct mixing method; ultraviolet conversion method [3, 4]. At present, WLEDs are fabricated by combining a blue LED chip GaN with yellow-emitting phosphor such as $Y_3Al_5O_{12}:Ce^{3+}$ [5]. However, this type of white light has low color rendering because of the deficiency in red region of the sunlight spectrum (above 600 nm). These shortcomings limit its prospects in the field of WLED lighting [6, 7]. Therefore, it is critical to add a red-emitting phosphor to compensate the deficiency [8–10].

Titanate system has excellent properties such as very good physical and chemical stability and being stably present in the epoxy resin or the like silicone encapsulating material; meanwhile rich resources of titanium lead to the clear price advantage compared with other molybdate and tungstate. It provides favorable conditions for the development of rare earth titanate functional materials. Figure 1 is the crystal structure of M_2TiO_4. Titanate M_2TiO_4 (M is generally alkaline earth metal or alkali metal and rare earth ion composition) basic phosphor is layered perovskite compound, among the perovskite layers is SrO layer, and Sr^{2+} ion is located among the perovskite layers, around which there are nine oxygen ligands [11, 12].

In this study, the $Sr_{2-x}Ba_xTiO_4:Eu^{3+}$, Gd^{3+} phosphors are synthesized by sol-gel method, with Eu^{3+} as activator and Gd^{3+} as sensitizer, and their luminescent properties were investigated. These phosphors were excited by blue chip and emit yellow light. Adjusting the ratio of blue and yellow light, more pure white light can be obtained, and the $Sr_{2-x}Ba_xTiO_4:Eu^{3+}$, Gd^{3+} phosphors are expected to be widely used in the WLED field [13, 14].

2. Experiment

2.1. Materials Preparation. The phosphor $Sr_{2-x}Ba_xTiO_4:Eu^{3+}$, Gd^{3+} was synthesized through the sol-gel method. All of the chemical reagents used in this experiment were of

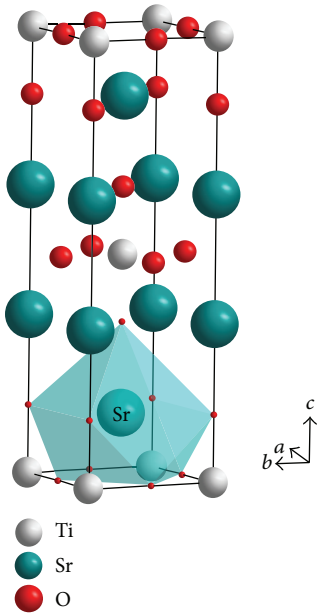

Figure 1: The crystal structure of M_2TiO_4.

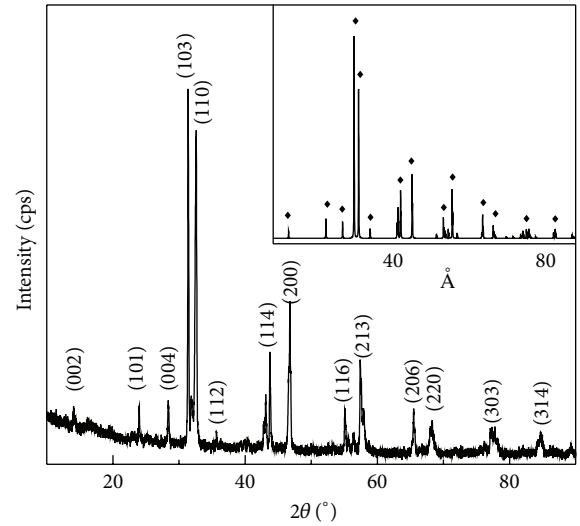

Figure 2: The XRD patterns of the $Sr_2TiO_4:Eu^{3+}$.

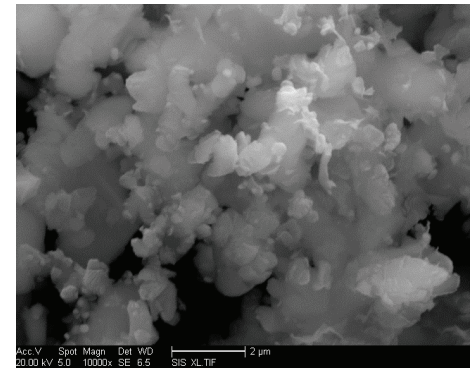

Figure 3: SEM image of the $Sr_2TiO_4:Eu^{3+}$.

analytical grade. An $Eu(NO_3)_3$ solution was prepared by dissolving Eu_2O_3 into the nitric acid. $Eu(NO_3)_3$, $Sr(NO_3)_2$, and $Ce(NO_3)_3$ solution were mixed in a stoichiometric ratio, followed by the addition of citric acid. Afterwards, tetrabutyl orthotitanate was slowly dropped into the mixture solution under constant stirring after being diluted by alcohol. The resulting mixture is placed into water bath at 80°C under stirring for 1 h until the gelation was completed. Then the yellow-green gel was placed in an oven at 80°C for 4 h. After drying process, a brown fluffy porous xerogel was obtained. Finally, the sample is calcined in a high temperature electronic furnace to obtain the desired phosphor.

2.2. Analysis Methods. The structure of the phosphor was established by X-ray diffractometer (XRD) (Shimadzu, XRD-6000, Cu Ka target) and the morphology of the particles was observed by field emission scanning electron microscope (FE-SEM) (Sirion 200, Philip). The photoluminescence properties of the phosphors were studied on fluorescence spectrophotometer (Shimadzu, model RF-5301 PC). All the photoluminescence properties of the phosphors were measured at room temperature.

3. Results and Discussion

3.1. Phase Characterization and SEM. To determine the phase purity of the samples, XRD measurements for the synthesized products were conducted. Figure 2 shows the XRD patterns of $Sr_2TiO_4:Eu^{3+}$, Gd^{3+}; Sr_2TiO_4 crystallizes in a tetragonal structure, with space group of I4mmm (number 139). The lattice parameters were determined to be $a = 3.8864$ Å and $c = 12.5934$ Å, which is in good agreement with JCPDS number 39-1471 ($a = 3.8861$ Å, $c = 12.5924$ Å). The ions radii of dopant element, Eu^{3+} (CN = 12, $r = 107$ pm), are expected to occupy the Sr^{2+} sites in the Sr_2TiO_4 host due to the close radii and identical valence of the ions. Figure 3 shows the SEM images of material calcined at 1100°C for 3 h, from which we can see the samples are single phase and have irregular shape.

3.2. The Luminescent Properties of $Sr_{2-x}Ba_xTiO_4:Eu^{3+}$, Gd^{3+}. The excitation spectra and emission spectra of $Sr_2TiO_4:Eu^{3+}$, Gd^{3+} phosphors are given in Figure 4. The excitation spectra were under 611 nm emission and the emission spectra were under 466 nm excitation. The excitation spectrum (curve a) extends at 393 nm and 466 nm, which is due to the transitions $^7F_0$-$^5L_6$ and $^7F_0$-$^5D_2$ of Eu^{3+}, respectively. The transition at 466 nm was the strongest absorption, which is corresponding to the excitation of blue chip. The $Sr_{2-x}Ba_xTiO_4:Eu^{3+}$, Gd^{3+} phosphor shows a yellow emission band peaking at 593 nm and 611 nm under 466 nm excitation (curve b), which are attributed to Eu^{3+} $^5D_0$-$^7F_1$, $^5D_0$-$^7F_2$, respectively.

In titanate phosphor, Eu^{3+} replaces the sites of Sr^{2+} as luminescent centers in matrix. When the amount of Eu^{3+} changes, the shape of emission spectra has no difference, but the intensity is changing. When the Eu^{3+} concentration

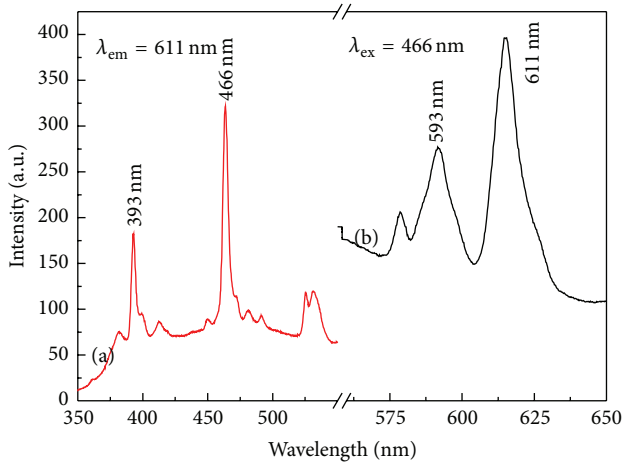

FIGURE 4: The excitation (λ_{em} = 611 nm) and emission (λ_{ex} = 466 nm) spectra of the Sr_2TiO_4:Eu^{3+} sample

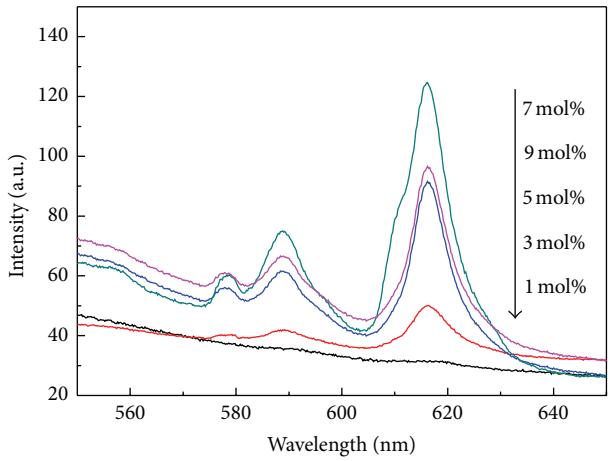

FIGURE 5: Emission spectra of different concentrations of Eu^{3+} doping.

increased, the emission intensity increased with the adding of emission center, especially notable for $^5D_0$-$^7F_2$ transition. However, when the doping content of Eu^{3+} continues to increase, the distance of activation centers is decreasing and nonradiative energy transfer between the matrix and the light-emitting center has become increasingly evident, leading to concentration quenching [15]. Thus the emission intensity decreased. Figure 5 is the emission spectra with the different doping concentrations of Eu^{3+}. The spectra indicate that the optimum doping concentration is 7%, corresponding to the strongest emission intensity.

The emission spectra with different Gd^{3+} doping amount are shown in Figure 6. As can be seen, the sample was under 466 nm excitation, and all the main emission peaks are attributed to Eu^{3+}, and the strongest peak is located at 611 nm. Compared to the single doped Eu^{3+}, the intensity of the emission peak at 611 nm has a significant enhancement compared to that at 593 nm, which is due to the addition of the symmetry of Gd^{3+} in crystal structure. When the

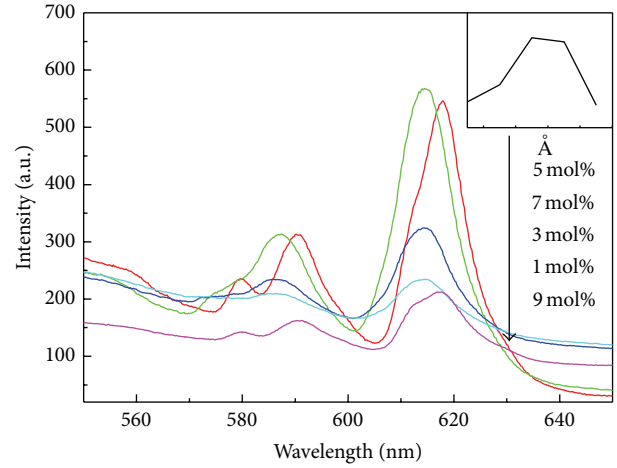

FIGURE 6: Emission spectra of different Gd^{3+} doping amount.

doping amount of Gd^{3+} was in a low level, the luminescence intensity enhances with the increase of the concentration of Gd^{3+}. Since the concentration increases to a certain value, energy transfer between the substrate and the sensitizer ions is then released in the form of heat or scattered in the form of nonradiation, thus leading to the reduction of the emission intensity. From Figure 6, it can be found that the optimum doping concentration is 5% corresponding to the strongest emission intensity.

3.3. Impact of Alkaline Earth Metal Doping. Crystal structure of the matrix material has a huge impact on the luminescent properties. With the change of the doping content of Ba^{2+}, the substitution of Ba^{2+} for Sr^{2+} has an impact on the phase. Figure 7 shows the XRD patterns of $Sr_{2-x}Ba_xTiO_4$:Eu^{3+} (Sr : Ba = 1 : 0, 4 : 1, 3 : 2, 2 : 3, 1 : 4), the standard Ba_2TiO_4 (38-1481), and Sr_2TiO_4 (39-1471). As can be seen, with the increasing of Ba^{2+} concentration, the crystalline phase of luminescent materials has a huge change. Since atomic radii of Ba^{2+} (1.35 Å) and Sr^{2+} (1.18 Å) are different, the substitution of Ba^{2+} for Sr^{2+} has impact on crystal structure; then the corresponding XRD patterns will change inevitably. With the increasing of Ba^{2+}, the diffraction peak owing to Sr_2TiO_4 becomes low and there are some miscellaneous peaks in the diffraction spectra. When the proportion of Sr and Ba reaches 2 : 3 and 3 : 2, the significant phase of Ba_2TiO_4 can be seen, that is, the phases of Sr_2TiO_4 and Ba_2TiO_4 coexistence. When the concentration of Ba^{2+} continues to increase, the phase of Ba_2TiO_4 is dominant, some weak peaks owing to Sr_2TiO_4 become acute again and even disappear, and the incorporation of rare earth Eu^{3+} into this lattice will result in various fluorescence characteristics depending on the different sites [16, 17].

Figure 8 shows the emission spectrum of $Sr_{2-x}Ba_xTiO_4$:Eu^{3+}, Gd^{3+}. The luminescence properties of two crystal phases are quite different with the content of the rare earth Eu^{3+}. We can see that, with the increasing concentration of Ba^{2+}, the emission intensity varies linearly

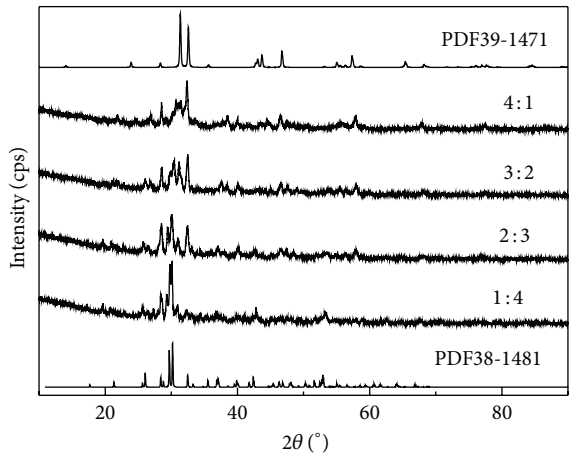

Figure 7: The XRD patterns of $Sr_{2-x}Ba_xTiO_4:Eu^{3+}$ (Sr : Ba = 1 : 0, 4 : 1, 3 : 2, 2 : 3, 1 : 4).

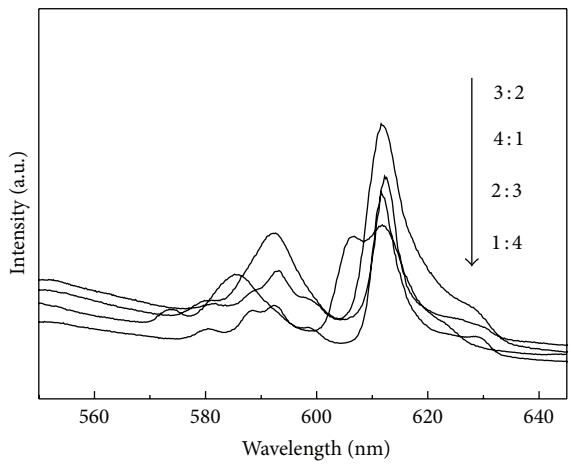

Figure 8: The emission spectrum of $Sr_{2-x}Ba_xTiO_4:Eu^{3+}$.

convexly, that is, because the addition of Ba^{2+} composed composite structure has a certain degree of enhancement of luminescence. However, when the crystalline phase of Ba_2TiO_4 dominates the emission intensity declined, this is mainly due to pure orthorhombic Ba_2TiO_4 which has no advantage on the luminescent of Eu^{3+}; there is also a significant blue-shift phenomenon in pure orthorhombic Ba_2TiO_4, which is consistent with the results reported in the literature [18]. When the ratio of Sr^{2+} and Ba^{2+} is 3 : 2, the optimum fluorescence property is obtained.

From Figure 8, we can see that the corresponding relative intensity of peaks at 593 and 611 nm has some changes. It is well known that the emission peak located at 593 nm and 611 nm is attributed to the transition of Eu^{3+} $^5D_0$-$^7F_1$ which is magnetic dipole transitions and $^5D_0$-$^7F_2$ which is electrical dipole transition, respectively. When the crystalline phase of Sr_2TiO_4 is dominant and the transition of $^5D_0$-$^7F_1$ is dominant, the lattice remains symmetric. However, with the increasing content of Ba, the symmetry of lattice structure has a great change. When Eu^{3+} substituted the position of Sr^{2+} or Ba^{2+}, the transition of $^5D_0$-$^7F_2$ is prominent. By adjusting the ratio of Sr and Ba combined, blue chip emitting can achieve desired white light.

4. Conclusions

A series of $Sr_{2-x}Ba_xTiO_4:Eu^{3+}$, Gd^{3+} was synthesized through the sol-gel method. The luminescent color ranges from yellow to red, and Eu^{3+} was used as activator and Gd^{3+} was used as sensitizer, aiming at increasing the luminous intensity. As the fluorescence properties are the best, the optimum doping concentration of Eu^{3+} and Gd^{3+} is 5% and 3%, respectively, and the optimum ratio of Sr and Ba is 3 : 2. When the phosphor combined a blue LED chip, the sample can be well applied to WLED.

Conflict of Interests

The authors declare that there is no conflict of interests regarding the publication of this paper.

Acknowledgment

This work was financially supported by Program for Innovative Research Team in the University of Heilongjiang (2013TD008).

References

[1] Y. Hu, W. Zhuang, H. Ye, S. Zhang, Y. Fang, and X. Huang, "Preparation and luminescent properties of $(Ca_{1-x},Sr_x)S:Eu^{2+}$ red-emitting phosphor for white LED," *Journal of Luminescence*, vol. 111, no. 3, pp. 139–145, 2005.

[2] H. Shono, T. Ohkawa, H. Tomoda, T. Mutai, and K. Araki, "Fabrication of colorless organic materials exhibiting white luminescence using normal and excited-state intramolecular proton transfer processes," *ACS Applied Materials and Interfaces*, vol. 3, no. 3, pp. 654–657, 2011.

[3] J. Yu, C. Guo, Z. Ren, and J. Bai, "Photoluminescence of double-color-emitting phosphor $Ca_5(PO_4)_3Cl:Eu^{2+}$, Mn^{2+} for near-UV LED," *Optics & Laser Technology*, vol. 43, no. 4, pp. 762–766, 2011.

[4] T. Kim and S. Kang, "Potential red phosphor for UV-white LED device," *Journal of Luminescence*, vol. 122-123, no. 1-2, pp. 964–966, 2007.

[5] X. C. Yan, R. B. Yu, Y. L. Xu et al., "Morphology-tailored synthesis of flower-like $Y_2O_3:Eu^{3+}$ microspheres," *Materials Research Bulletin*, vol. 47, no. 9, pp. 2135–2139, 2012.

[6] A. A. Setlur, W. J. Heward, Y. Gao, A. M. Srivastava, R. Gopi Chandran, and M. V. Shankar, "Crystal chemistry and luminescence of Ce^{3+}-doped $Lu_2CaMg_2(Si,Ge)_3O_{12}$ and its use in LED based lighting," *Chemistry of Materials*, vol. 18, no. 14, pp. 3314–3322, 2006.

[7] X. Piao, K.-I. Machida, T. Horikawa, H. Hanzawa, Y. Shimomura, and N. Kijima, "Preparation of $CaAlSiN_3:Eu^{2+}$ phosphors by the self-propagating high-temperature synthesis and their luminescent properties," *Chemistry of Materials*, vol. 19, no. 18, pp. 4592–4599, 2007.

[8] H. Shabir, B. Lal, and M. Rafat, "Sol-gel synthesis of Eu^{3+}: $Tb_3Al_5O_{12}$ nanophosphor," *Journal of Sol-Gel Science and Technology*, vol. 53, no. 2, pp. 399–404, 2010.

[9] Y. Zorenko, V. Gorbenko, T. Voznyak et al., "Luminescence properties of phosphors based on $Tb_3Al_5O_{12}$ (TbAG) terbium-aluminum garnet," *Optics and Spectroscopy*, vol. 106, no. 3, pp. 365–374, 2009.

[10] Y. Shimomura, T. Kurushima, M. Shigeiwa, and N. Kijima, "Redshift of green photoluminescence of $Ca_3Sc_2Si_3O_{12}$:Ce^{3+} phosphor by charge compensatory additives," *Journal of the Electrochemical Society*, vol. 155, no. 2, pp. J45–J49, 2008.

[11] Y. Inaguma, D. Nagasawa, and T. Katsumata, "Photoluminescence of praseodymium-doped $Sr_{n+1}Ti_nO_{3n+1}$($n = 1, 2, \infty$)," *Japanese Journal of Applied Physics*, vol. 44, no. 1S, pp. 761–765, 2005.

[12] Z. Lu, L. Zhang, N.-C. Xu, L.-X. Wang, and Q.-T. Zhang, "Luminescent properties of Eu^{3+} doped layered perovskite structure M_2TiO_4(M = Ca, Sr, Ba) red-emitting phosphors," *Spectroscopy and Spectral Analysis*, vol. 32, no. 10, pp. 2632–2636, 2012.

[13] J. K. Park, C. H. Kim, S. H. Park, H. D. Park, and S. Y. Choi, "Application of strontium silicate yellow phosphor for white light-emitting diodes," *Applied Physics Letters*, vol. 84, no. 10, pp. 1647–1649, 2004.

[14] Y.-F. Wu, Y.-H. Chan, Y.-T. Nien, and I.-G. Chen, "Crystal structure and optical performance of Al^{3+} and Ce^{3+} codoped $Ca_3Sc_2Si_3O_{12}$ green phosphors for white LEDs," *Journal of the American Ceramic Society*, vol. 96, no. 1, pp. 234–240, 2013.

[15] M. J. Weber, "Nonradiative decay from 5d states of rare earths in crystals," *Solid State Communications*, vol. 12, no. 7, pp. 741–744, 1973.

[16] V. Sivakumar and U. V. Varadaraju, "A promising orange-red phosphor under near UV excitation," *Electrochemical and Solid-State Letters*, vol. 9, no. 6, pp. H35–H38, 2006.

[17] G. Blasse and L. H. Brixner, "A comparison between the Gd^{3+} emission in the scheelite structure and the M-$YTaO_4$ structure," *Journal of Solid State Chemistry*, vol. 82, no. 1, pp. 151–155, 1989.

[18] E. Korkmaz, N. O. Kalaycioglu, and V. E. Kafadar, "Yellow phosphors doping with Gd^{3+}, Tb^{3+} and Lu^{3+} in $MTiO_3$ (M = Mg and Sr) luminescence properties," *Bulletin of Materials Science*, vol. 36, no. 6, pp. 1079–1086, 2013.